



OPEN

SUBJECT AREAS:
CANCER THERAPEUTIC
RESISTANCE
BREAST CANCER

Received
9 September 2013

Accepted
31 March 2014

Published
16 April 2014

Correspondence and
requests for materials
should be addressed to
E.V.D. (d_evgeniy@
oncology.tomsk.ru)

* These authors
contributed equally to
this work.

Intratumoral morphological heterogeneity of breast cancer: neoadjuvant chemotherapy efficiency and multidrug resistance gene expression

Evgeny V. Denisov^{1,2*}, Nikolay V. Litviakov^{1,2*}, Marina V. Zavyalova^{2,3,4}, Vladimir M. Perelmuter^{3,4}, Sergey V. Vtorushin^{3,4}, Matvey M. Tsyganov^{1,2}, Tatiana S. Gerashchenko^{1,2}, Evgeny Yu. Garbukov⁵, Elena M. Slonimskaya^{5,6} & Nadezhda V. Cherdyntseva^{1,2,6}

¹Department of Experimental Oncology, Cancer Research Institute, Siberian Branch of the Russian Academy of Medical Sciences, Tomsk, Russian Federation, ²Laboratory of Translational Cell and Molecular Biomedicine, Tomsk State University, Tomsk, Russian Federation, ³Department of Pathological Anatomy and Cytology, Cancer Research Institute, Siberian Branch of the Russian Academy of Medical Sciences, Tomsk, Russian Federation, ⁴Department of Pathological Anatomy, Siberian State Medical University, Tomsk, Russian Federation, ⁵Department of General Oncology, Cancer Research Institute, Siberian Branch of the Russian Academy of Medical Sciences, Tomsk, Russian Federation, ⁶Department of Oncology, Siberian State Medical University, Tomsk, Russian Federation.

In this study, the influence of intratumoral morphological heterogeneity of breast cancer on neoadjuvant chemotherapy (NAC) efficiency was investigated. In particular, we analysed the association of NAC response and pre- and post-NAC expression of the main multidrug resistance (MDR) genes - *ABCB1*, *ABCC1*, *ABCC5*, *ABCG1*, and *ABCG2*, with the presence of different morphological structures in breast tumors. In addition, the expression of MDR genes was investigated in different morphological structures and in their microenvironment by comparing probes obtained using laser microdissection. The results of this study showed that tumors with alveolar structures were more frequently NAC-nonresponsive than cases without this structural type ($p = 0.0028$, Bonferroni-corrected $p = 0.014$). The presence of trabecular structures in breast tumors was also associated with chemoresistance ($p = 0.0272$, Bonferroni-corrected $p = 0.136$). High expression of MDR genes was not found in alveolar structures (including their microenvironment) and in tumors containing this structural type. In contrast, more active MDR genes and expression of the *ABCB1* gene were found only in trabecular structures. Taken together, our data indicate that breast tumors with alveolar structures possess resistance to NAC, which is not related to high expression of MDR genes, whereas chemoresistance of tumors with trabecular structures can depend on the expression level of *ABCB1*.

Breast cancer is a complex disease with high inter- and intratumoral heterogeneity^{1,2}. Invasive carcinoma of no special type (IC NST)³, previously classified as invasive ductal carcinoma, not otherwise specified (NOS)⁴, account for a substantial proportion (up to 75%) of breast cancer cases and display extremely diverse morphological characteristics that make these tumors difficult to classify histologically⁵. IC NST tumors often contain minor components of special types of histology, including architectural features of the invasive process, which may vary widely both within a single tumor and from case to case⁶. Previously, we have described five different types of invasive component or morphological structures in IC NST tumors - tubular, trabecular, solid, alveolar structures, and discrete groups of tumor cells⁷ - and found that such intratumoral morphological heterogeneity was related to cancer metastasis^{7,8}. In addition, our recent data provided evidence that phenotypic drift can be cause of the development of intratumoral morphological heterogeneity in IC NST⁹.

At present, the study of intratumoral heterogeneity appears to be key for the development of personalized approaches in cancer treatment^{10,11}. In 2008, we reported that intratumoral morphological heterogeneity of IC


Table 1 | The clinicopathological parameters of BC patients, n = 382

Clinicopathological parameter		N (%)
Age (year)	≤50	221 (57.9)
	>50	161 (42.1)
Menstrual status	Pre	188 (49.2)
	Post	194 (50.8)
Tumor size	T ₁	102 (26.7)
	T ₂	239 (62.5)
	T ₃	35 (9.2)
	T ₄	6 (1.6)
Lymph node status	N ₀	176 (46.1)
	N ₁	122 (31.9)
	N ₂	78 (20.4)
	N ₃	6 (1.6)
Estrogen receptor	Positive	146 (38.2)
	Negative	136 (35.6)
	No data	100 (26.2)
Progesterone receptor	Positive	150 (39.3)
	Negative	132 (34.5)
	No data	100 (26.2)
HER2	0	219 (57.3)
	1+	36 (9.4)
	2+	16 (4.3)
	3+	36 (9.4)
	No data	75 (19.6)
Histological form	Unicentric	322 (84.3)
	Multicentric	60 (15.7)
NAC regimen	CAX	114 (29.9)
	FAC	206 (53.9)
	Taxotere	62 (16.2)
NAC response	Complete response	0 (0)
	Partial response	169 (44.2)
	Stable disease	202 (52.9)
	Progressive disease	11 (2.9)

All patients had invasive carcinoma of no special type. Abbreviations: NAC, neoadjuvant chemotherapy; CAX, Cyclophosphamide-Adriamycin-Xeloda; FAC, 5-Fluorouracil-Adriamycin-Cyclophosphamide; HER2 testing is performed in accordance with American Society of Clinical Oncology/College of American Pathologists Guideline 2007 Recommendation⁴⁸.

NST was associated with the efficiency of neoadjuvant chemotherapy (NAC): the presence of alveolar and trabecular structures in breast tumors resulted in a poor response to NAC¹². The mechanisms involved in drug resistance of heterogeneous tumors are not completely established. It is reasonable to assume that tumors contain different clones of tumor cells with different degrees of responsiveness to chemotherapy. Various molecular factors can be involved in tumor drug resistance, mainly ATP-binding cassette (ABC) trans-

porters, which are encoded by a large family of multidrug resistance (MDR) genes and play a major role in mediating drug resistance¹³. In this study, we focused on the key MDR genes - *ABCB1*, *ABCC1*, *ABCC5*, *ABCG1*, and *ABCG2*.

Thus, on a larger scale than in our previous research¹², we aimed to study the association between the NAC response and the presence of different types of morphological structures in IC NST tumors. Then, we investigated pre- and post-NAC expression levels of the MDR genes in breast tumors and whether they depend on the presence of various morphological structures. Finally, using laser microdissection we estimated expression levels of the MDR genes directly in different morphological structures and in their microenvironment.

Results

Analysis of correlation of intratumoral morphological heterogeneity of IC NST and NAC response. Using hematoxylin & eosin staining and morphological analysis, we identified different morphological structures in breast tumors (n = 382; patient characteristics are listed in Table 1). Statistical analysis of the association between NAC response and the presence/absence of different morphological structures in breast tumors was conducted using Pearson's chi-square test with Bonferroni correction (Table 2). Patients with alveolar structures were more frequently NAC-nonresponsive than were cases without this structural type (61.9% vs. 46.4%; p = 0.0028, Bonferroni-corrected p = 0.014). In addition, breast tumors with trabecular structures more often demonstrated chemotherapy resistance as compared with tumors without these structures (58.8% vs. 45.3%; p = 0.0272). However, the difference did not reach statistical significance after Bonferroni correction (p = 0.136).

Analysis of correlation of intratumoral morphological heterogeneity of IC NST and expression of MDR genes. Using RT-PCR, we have compared the expression levels of MDR genes in the pre- and post-NAC tumor samples (n = 69) with the presence/absence of different morphological structures. Statistical analysis of the correlation of gene expression with different morphological structures of tumor was performed using logistic regression with Bonferroni correction. Expression of *ABCB1* (p = 0.007) and *ABCC5* (p = 0.027) genes was significantly lower in post-NAC tumors with tubular structures compared with tumors without tubular structures. Patients with solid structures displayed a decreased post-NAC expression of *ABCB1* (p = 0.011) and *ABCG2* (p = 0.002) genes in comparison with patients whose tumors did not contain the solid structures. However, the differences in the expression of *ABCB1* and *ABCG2* were not significant after Bonferroni correction (p > 0.05; Table 3). In Tables 4 and 5, we showed the results of analysis of MDR gene expression in the distinct morphological

Table 2 | The response to neoadjuvant chemotherapy depending on the presence of different types of morphological structures in breast tumors

		n	PR N (%)	SD + PD N (%)	Uncorrected p value	Corrected p value*
Alveolar structures	no	151	81 (53.6)	70 (46.4)	0.0028	0.014
	yes	231	88 (38.1)	143 (61.9)		
Trabecular structures	no	86	47 (54.7)	39 (45.3)	0.0272	0.136
	yes	296	122 (41.2)	174 (58.8)		
Tubular structures	no	248	111 (44.8)	137 (55.2)	0.7819	NA
	yes	134	58 (43.3)	76 (56.7)		
Solid structures	no	225	102 (45.3)	123 (54.7)	0.6068	NA
	yes	157	67 (42.7)	90 (57.3)		
Discrete groups of tumor cells	no	155	68 (43.9)	87 (56.1)	0.9043	NA
	yes	227	101 (44.5)	126 (55.5)		

Statistical analysis: p value, Pearson's chi-squared test;

*, Bonferroni-corrected p value was calculated as the each p value multiplied by the number of tests (n = 5).

Abbreviations: n, number of patients with presence (yes) or absence (no) of any morphological structures; N, number of patients with presence/absence of any morphological structures possessing response/non-response to neoadjuvant chemotherapy; PR, partial response; SD, stable disease; PD, progressive disease; NA, not applied.



Table 3 | The link of pre- and post-NAC expression levels of MDR genes with the presence/absence of different types of morphological structures in breast tumors

Gene expression	Alveolar structures		Trabecular structures		Tubular structures		Solid structures		Discrete groups of tumor cells		
	no	yes	no	yes	no	yes	no	yes	no	yes	
ABCB1	pre-NAC	4.17 ± 1.31	4.78 ± 1.29	2.77 ± 0.79	5.21 ± 1.29	6.84 ± 1.97	3.09 ± 0.95	4.73 ± 1.22	4.51 ± 1.52	5.94 ± 2.30	3.99 ± 1.00
	post-NAC	4.63 ± 1.44	5.72 ± 1.39	4.10 ± 1.32	5.85 ± 1.37	8.72 ± 2.31	3.16 ± 0.74 ¹	8.20 ± 2.16	3.15 ± 0.70 ³	6.07 ± 1.58	5.12 ± 1.41
ABCC1	pre-NAC	1.12 ± 0.18	1.60 ± 0.31	0.93 ± 0.12	1.64 ± 0.30	1.40 ± 0.24	1.51 ± 0.36	1.51 ± 0.36	1.43 ± 0.31	2.02 ± 0.57	1.21 ± 0.21
	post-NAC	1.13 ± 0.24	2.80 ± 1.12	1.25 ± 0.34	2.70 ± 1.07	3.56 ± 1.94	1.52 ± 0.36	3.21 ± 1.75	1.64 ± 0.40	1.38 ± 0.25	2.80 ± 1.19
ABCC5	pre-NAC	3.00 ± 0.91	2.74 ± 0.34	3.19 ± 1.03	2.69 ± 0.32	3.22 ± 0.75	2.56 ± 0.33	3.08 ± 0.61	2.60 ± 0.41	3.60 ± 0.62	2.44 ± 0.42
	post-NAC	2.53 ± 0.51	3.75 ± 0.71	4.67 ± 1.70	2.98 ± 0.42	4.80 ± 1.23	2.52 ± 0.34 ²	3.79 ± 0.64	3.09 ± 0.82	4.85 ± 1.36	2.70 ± 0.41
ABCG1	pre-NAC	2.82 ± 1.03	1.98 ± 0.62	2.61 ± 0.78	2.09 ± 0.65	2.80 ± 1.06	1.82 ± 0.52	2.36 ± 0.93	2.10 ± 0.59	2.44 ± 1.31	2.12 ± 0.50
	post-NAC	1.39 ± 0.60	1.83 ± 0.48	1.52 ± 0.43	1.76 ± 0.49	1.59 ± 0.57	1.78 ± 0.52	1.53 ± 0.66	1.85 ± 0.44	1.36 ± 0.30	1.86 ± 0.54
ABCG2	pre-NAC	2.77 ± 0.70	2.50 ± 0.44	1.89 ± 0.56	2.79 ± 0.46	3.17 ± 0.66	2.16 ± 0.43	2.84 ± 0.53	2.35 ± 0.53	2.47 ± 0.71	2.62 ± 0.44
	post-NAC	3.35 ± 0.84	2.71 ± 0.48	3.61 ± 0.89	2.65 ± 0.47	3.79 ± 0.68	2.27 ± 0.52	4.22 ± 0.78	1.81 ± 0.34 ⁴	3.80 ± 0.89	2.46 ± 0.45

Statistical analysis: Logistic regression was applied to identify differences between pre-NAC expression levels and between post-NAC expression levels depending on the presence/absence of different types of morphological structures.

¹, $p = 0.007$ (Bonferroni-corrected $p = 0.35$);

², $p = 0.027$ (Bonferroni-corrected $p = 1.00$);

³, $p = 0.011$ (Bonferroni-corrected $p = 0.55$);

⁴, $p = 0.002$ (Bonferroni-corrected $p = 0.10$). The Bonferroni-correction was calculated as the each p value multiplied by the number of tests ($n = 50$).

Abbreviations: no, the absence of any morphological structures; yes, the presence of any morphological structures; expression levels are shown as mean and standard error ($M \pm SE$).

structures and in their microenvironment of two breast tumors obtained by laser microdissection. Tissue sections before and after laser microdissection are shown in Figure 1. In trabecular structures, we detected the expression of the most MDR genes. Most importantly, expression of *ABCB1* gene was specific only for trabecular structures. In contrast, alveolar structures displayed a low expression of MDR genes. Interestingly, the microenvironment of different morphological structures also demonstrated expression of MDR genes, although in most cases gene activity was less than in morphological structures.

Analysis of correlation of intratumoral morphological heterogeneity of IC NST and up-/downregulation of MDR genes during NAC. We performed the quantitative analysis of the MDR gene expression changes during NAC in breast tumors with different morphological structures. For this purpose, frequencies of the increase or decrease in MDR gene expression during NAC were compared between patients with the presence or absence of different morphological structures using Pearson's chi-square test with Bonferroni correction (Table 6). A decrease in *ABCB1* expression was more frequently detected in breast tumors with solid structures in comparison with tumors without this structural type (63% versus 35%, $p = 0.022$). Similarly, we frequently observed *ABCG2* downregulation in cases with discrete groups of tumor cells than in patients whose tumors were free from these morphological structures (66% versus 32%, $p = 0.008$). However, the statistical significance of the differences was not confirmed after Bonferroni correction ($p > 0.05$).

Discussion

In this study, we demonstrated that intratumoral morphological heterogeneity of breast cancer, which was previously described in the most common histological type - invasive carcinoma of no special type⁷, influences the efficiency of neoadjuvant chemotherapy. On a larger scale than our previous study¹², we confirmed, with greater statistical significance, the association between the presence of alveolar structures in breast tumors and poor NAC response, which was significant after Bonferroni correction. In addition, trabecular structures were also related to chemotherapy resistance as previously suggested¹²; however, the Bonferroni correction did not show the significance of this association.

Chemotherapy efficiency is composed of many host factors and tumor alterations¹⁴. The most common reason for cancer drug resistance is the expression of one or more ATP-binding cassette transporters that detect and eject anticancer drugs from tumor cells^{13,14}. The data of our previous study suggest that changes in expression of MDR genes during the chemotherapy process or the development of adaptive MDR, but not the mRNA levels of these genes per se, are associated with NAC efficiency. In particular, reduction in MDR gene expression in post-NAC samples in comparison with pre-NAC tumors was linked with good response to chemotherapy, whereas patients displaying MDR gene upregulation exhibited resistance to therapy¹⁵. In addition, recent data indicate that chemotherapy-induced upregulation of MDR genes can result in decreased distant metastasis¹⁶ and disease-free¹⁷ survival.

The data obtained in this study suggested that chemoresistance of breast tumors with trabecular structures is associated with high levels of expression of MDR genes. Trabecular structures showed more active MDR genes. In addition, only trabecular structures were found to express the *ABCB1* gene encoding P-glycoprotein, which is broad-spectrum drug efflux pump and plays a central role in MDR¹⁴. This is in consistency with our published study performed on the basis of FFPE tumor material¹⁸. Interestingly, an increased expression of MDR genes both before and after NAC, and their upregulation during chemotherapy were not found in breast tumors with trabecular structures.


Table 4 | Expression levels of MDR genes in different types of morphological structures and in their microenvironment of the first breast tumor

Genes	Alveolar structures		Trabecular structures		Solid structures		Discrete groups of tumor cells	
		ME		ME		ME		ME
<i>ABCB1</i>	0	0	0.122	0	0	0	0	0
<i>ABCC1</i>	0.299	0	0.001	0	1.303	0	0.126	10.464
<i>ABCC5</i>	0.034	0	0.004	0	6.189	0.003	2.038	21.594
<i>ABCG1</i>	0.002	0	5.351	0.0004	0.340	0	6.386	0
<i>ABCG2</i>	0	0	0.002	0	0	0	301.593	0

Abbreviations: ME, microenvironment.

In contrast, poor response of breast tumors with alveolar structures to NAC seems not to correlate to MDR gene activity. In particular, tumors with alveolar structures did not show high expression of MDR genes both before and after NAC. Moreover, MDR gene upregulation was also absent in these tumors. In addition, laser microdissection-based expression analysis showed a low activity of MDR genes in alveolar structures. Previously, MDR genes and ABC transporters were found to be expressed in different cells of the tumor stroma^{19–21}. However, we showed almost complete absence of MDR gene activity in the microenvironment of alveolar structures.

Alveolar structures have spheroid shapes containing 10–30 tumor cells. During the 1970s, it was shown *in vitro* that multicellular spheroids containing thousands of cells were more resistant to radiation and adriamycin than cells cultured in a monolayer^{22,23}. Additionally, smaller spheroids consisting of 5–50 cells were also found to be more chemoresistant than single cells or monolayer cultures^{24,25}. This phenomenon was later termed “multicellular resistance (MCR)”²⁶, which was linked to insensitivity to almost all anticancer drugs²⁷. Subsequent studies reported that MCR mechanisms are associated with the inability of the drug to penetrate the spheroid, differences in cell cycle distribution within spheroid, the presence of hypoxic cells, apoptosis inhibition, an increased DNA repair capacity, the so-called “contact effect”, and others^{25,27,28}. In addition, formation of tumor spheroids is a hallmark *in vitro* of cancer stem cells, and these tumor-initiating cells demonstrate increased drug resistance and prolonged survival²⁹.

P-glycoprotein acts more efficiently in tumor spheroids than in monolayer cultures because of upregulation of the *ABCB1* gene by hypoxia and acidification, which are attributes of tumor spheres³⁰. For instance, Doublier et al. showed that tumor spheroids obtained from MCF7 breast cancer cells were resistant to doxorubicin, and this resistance was associated with an increased P-glycoprotein expression via activation of hypoxia-inducible factor-1 (HIF-1)³¹. Based on the similarity between MCF7 spheroids and clusters of tumor cells of invasive micropapillary carcinoma (IMPC) of the breast, it has been hypothesized that chemoresistance of this subtype of breast cancer is provoked by high activity of P-glycoprotein³¹. IMPC clusters and alveolar structures of IC NST seem to have similar morphology. Moreover, micropapillary foci can be found in IC NST³². Results of our study demonstrate that high expression and upregulation of *ABCB1* gene are not common for alveolar structures and breast tumors containing this morphological variant. The differences in

chemoresistance mechanisms of IMPC clusters and IC NST alveolar structures probably reflect specific but not identified yet biological features of these groups of tumor cells. IMPC clusters detach from the stroma and display aberrant localization of glycoprotein MUC-1 (also known as epithelial membrane antigen, EMA) at the stromal-basal surface, corresponding to an inversion of cell polarity^{31,33}. In contrast, immunohistochemical analysis of two IC NST cases used in laser microdissection of the present study showed that in alveolar structures expression of MUC-1 (EMA) is observed in the whole cytoplasmic membrane and/or cytoplasm. In addition, in alveolar structures the change of cell polarization is not found, although the loss of interaction with stroma sometimes occurs (Fig. 2). It should be also pointed out that in IC NST, the frequency of alveolar structures comprises 60–83% (our unpublished data), whereas the proportion of micropapillary foci constitutes only 7.0%³².

It is interesting to note that tumor spheroids (microemboli) were previously detected in peripheral blood of patients with lung^{34–36}, prostate^{36,37}, renal cell³⁸, colorectal^{39,40}, and breast⁴¹ carcinoma. In comparison with circulating single tumor cells, such tumor clusters were shown to have anoikis suppression and the highest metastatic potential³⁵. In addition, it has been suggested that the lack of apoptosis and perhaps proliferation make tumor clusters more resistant to chemotherapy than solitary tumor cells⁴².

Overall, our data confirm that intratumoral morphological heterogeneity of invasive carcinoma of no special type is related to NAC efficiency. Breast tumors containing alveolar structures demonstrate a poor response to NAC and such observation is not explained by initial and adaptive MDR or upregulation of MDR genes during chemotherapy. In addition, the presence of trabecular structures in breast tumors is also associated with chemoresistance probably via *ABCB1* expression (P-glycoprotein). Further studies are needed to investigate what factors/mechanisms are involved in chemoresistance of breast tumors with trabecular and alveolar structures.

Methods

Patients, tumors, and treatments. Patients (n = 382) with clinical stage IIA to IIIC ($T_{1-4}N_{0-3}M_0$) IC NST, between 25 and 71 years of age (mean age: 51.9 ± 0.50), and treated in the Cancer Research Institute (Tomsk, Russia) between 2006 and 2012 were included (Table 1). The procedures followed in this study were in accordance with the Helsinki Declaration (1964, amended in 1975 and 1983). This study was approved by the institutional review board, and all patients signed an informed consent for voluntary participation. All patients received two to four preoperative cycles of FAC (5-Fluorouracil, Adriamycin, and Cyclophosphamide), CAX (Cyclophosphamide, Adriamycin, Xeloda) regimen, or Taxotere. Physical examination was performed

Table 5 | Expression levels of MDR genes in different types of morphological structures and in their microenvironment of the second breast tumor

Genes	Alveolar structures		Trabecular structures		Solid structures		Discrete groups of tumor cells	
		ME		ME		ME		ME
<i>ABCB1</i>	0	0	2.210	0	0	0	0	0
<i>ABCC1</i>	0	0	0	0	0	0	0	0
<i>ABCC5</i>	0.157	0	0	0.068	1260.523	0.543	0	0.181
<i>ABCG1</i>	0.465	0.003	0.066	0.001	3.437	0.038	0.739	0.053
<i>ABCG2</i>	0	0	21.360	0	0	0	29.912	0

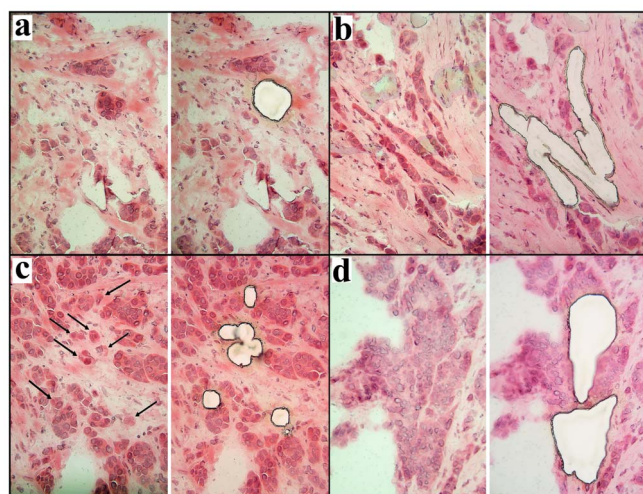


Figure 1 | Laser microdissection of different types of morphological structures from sections of breast tumor. (a), alveolar structure; (b), trabecular structures; (c), discrete groups of tumor cells (marked by arrows); (d), solid structures. 200 \times magnification.

before NAC and was repeated after 2 cycles of NAC and before surgery to determine clinical response. Imaging of the primary breast lesion was performed with mammography and/or ultrasonography. Clinical and imaging responses to NAC were categorized into the following groups according to the International Union Against Cancer criteria⁴³: complete response (CR), partial response (PR), stable disease (SD), and progressive disease (PD). Patients were grouped into clinical responders (PR) and non-responders (SD and PD). Fresh tumor tissues ($n = 382$) obtained after NAC were fixed in 10% neutral formalin (Karbolit, Russia) for 24 hours, rinsed with an isopropanol solution (Biovitrum, Russia), and embedded in paraffin (Biovitrum, Russia). In addition, out of 382 fresh tumor samples, 69 (randomly selected) samples and their biopsies (before NAC) were placed in RNA-later solution (Ambion, USA) and were stored at -80°C until RNA isolation. The operative samples from two patients without NAC were collected after surgery in nitrogen and were stored at -80°C until laser microdissection. Cases with CR were excluded from this study because of a loss of post-NAC tumor samples for expression analysis.

Morphological analysis. Morphological analysis included identification of different morphological structures in breast tumors and was performed by light microscope (Axio Scope, Carl Zeiss, Germany). The presence of tubular, trabecular, solid, alveolar structures, and discrete groups of tumor cells was evaluated in breast tumors ($n = 382$) using 5 μm -thick tumor sections stained by hematoxylin (Dako, Denmark) and eosin (Dako, Denmark). All tumor slides (five from each sample) were reviewed by three experienced pathologists. Tubular structures used in tumor grading were identified as rows of tiny tube-shaped cell aggregations. Trabecular structures were

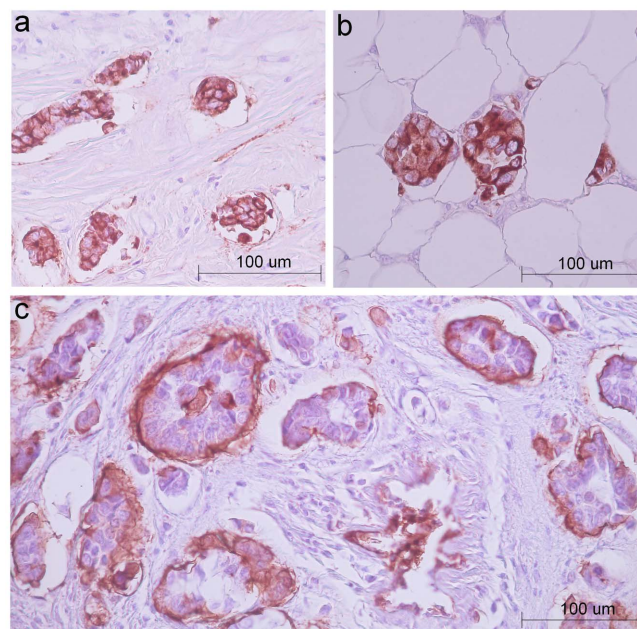


Figure 2 | Immunohistochemical staining for EMA in alveolar structures and papillary clusters of tumor cells. (a), (b): two cases with IC NST used in laser microdissection are shown. Alveolar structures of IC NST display the whole cytoplasmic membrane and/or cytoplasm expression of EMA (bar 100 microns). (c): one case with micropapillary foci in IC NST is presented to illustrate EMA expression the stromal-basal surface of papillary clusters of tumor cells and an inversion of cell polarity (bar 100 microns). NCL-EMA antibody (clone GP1.4, Novocastra) was used.

formed by two or more rows of cells. Solid structures represented groups of hundreds of cells with different sizes and shapes. Discrete groups of tumor cells were detected as single cells or as groups of up to five cells. Alveolar structures with rounded shapes contained 10–30 cells. It is important to note that tumors from different patients may have different types of morphological structures. Detailed descriptions and images of different types of morphological structures were presented in our previous paper⁷.

RNA isolation and cDNA synthesis. Total RNA was extracted from 69 samples of pre- and post-NAC tumor tissues using the RNeasy Mini Kit Plus DNase I digestion (Qiagen, Germany). Ribolock RNase inhibitor (Fermentas, Lithuania) was added to the isolated RNA. To assess RNA integrity, RIN was measured using 2200 TapeStation Instrument and R6K ScreenTape (Agilent Technologies, Inc., Santa Clara, USA). RNA with RIN > 6 was reverse transcribed to cDNA using the

Table 6 | The relationship between changes in MDR gene expression and presence/absence of different types of morphological structures in breast tumors

		n1/n2 (%/%)				
		ABCB1	ABCC1	ABCC5	ABCG1	ABCG2
Alveolar structures	no	7/12 (37/63)	9/10 (47/53)	10/9 (53/47)	5/14 (26/74)	7/12 (37/63)
	yes	27/23 (54/46)	27/23 (54/46)	25/23 (52/48)	21/27 (44/56)	24/26 (48/52)
Trabecular structures	no	9/8 (53/47)	10/7 (59/41)	10/7 (59/41)	7/9 (44/56)	10/7 (59/41)
	yes	25/27 (48/52)	26/26 (50/50)	25/25 (50/50)	19/32 (37/63)	21/31 (40/60)
Tubular structures	no	15/13 (54/46)	15/13 (54/46)	13/13 (50/50)	11/16 (41/59)	12/16 (43/57)
	yes	19/22 (46/54)	21/20 (51/49)	22/19 (54/46)	15/25 (38/62)	19/22 (46/54)
Solid structures	no	20/11 ¹ (65/35)	17/14 (55/45)	18/12 (60/40)	11/20 (35/65)	17/14 (55/45)
	yes	14/24 ¹ (37/63)	19/19 (50/50)	17/20 (46/54)	15/21 (42/58)	14/24 (37/63)
Discrete groups of tumor cells	no	14/8 (64/36)	10/12 (45/55)	13/9 (59/41)	10/11 (48/52)	15/7 ² (68/32)
	yes	20/27 (43/57)	26/21 (55/45)	22/23 (49/51)	16/30 (35/65)	16/31 ² (34/66)

Statistical analysis: Pearson's chi-squared test was used to detect significance of relationship between changes in MDR gene expression and the presence/absence of different types of morphological structures.

¹, $p = 0.022$ (Bonferroni-corrected $p = 0.55$);

², $p = 0.008$ (Bonferroni-corrected $p = 0.2$). The Bonferroni-correction was calculated as the each p value multiplied by the number of tests ($n = 25$).

Abbreviations: n1, number of patients with increase in gene expression after neoadjuvant chemotherapy; n2, number of patients with decrease in gene expression after neoadjuvant chemotherapy; no, the absence of any morphological structures; yes, the presence of any morphological structures.



RevertAid Kit with random hexanucleotide primers (Fermentas, Lithuania) following the manufacturer's instructions.

Laser microdissection. Frozen tumor samples from two untreated patients with IC NST were used for PALM MicroBeam laser capture microdissection (Carl Zeiss, Germany). Alveolar, trabecular, solid structures, and discrete groups of tumor cells were isolated from 5 μm -thick sections stained by hematoxylin (Dako, Denmark) and eosin (Dako, Denmark) (Fig. 1). In addition, the microenvironment of these structures was also isolated. Note that tumors of these patients did not contain tubular structures. The microdissected material was collected in RLT lysis buffer (RNeasy Plus Micro Kit, Qiagen, USA), and RNA was extracted according to the manufacturer's instructions. Ribolock RNase inhibitor (Fermentas, Lithuania) was added to the isolated RNA. RIN was measured using 2200 TapeStation Instrument and High Sensitivity R6K ScreenTape (Agilent Technologies, Inc., Santa Clara, USA). cDNA was synthesized, ligated, and amplified using a QuantiTect Whole Transcriptome Kit (Qiagen, USA) according to the manufacturer's instructions.

Expression analysis. The expression levels of the MDR genes were measured by quantitative real-time PCR (qRT-PCR) based on TaqMan technology using a Rotor-Gene-6000 instrument (Corbett Research, Australia). qRT-PCR was performed in triplicate reactions in a volume of 15 μl containing 250 μM dNTPs (Sibenzyme, Russia), 300 nM forward and reverse primers, 200 nM probe, 2.5 mM MgCl_2 , $1 \times \text{SE}$ buffer (67 mM Tris-HCl pH 8.8 at 25°C, 16.6 mM $(\text{NH}_4)_2\text{SO}_4$, 0.01% Tween-20), 2.5 U Hot Start Taq polymerase (Sibenzyme, Russia), and 50 ng of template cDNA. Samples were heated for 10 min at 95°C followed by 40 cycles of amplification for 10 s at 95°C and 20 s at 60°C. The primer and probe sequences of *ABCB1*, *ABCC1*, *ABCC5*, and *ABCG2* were given in our previous study¹⁵. The primer and probe sequences of *ABCG1* were obtained from a previous paper⁴⁴. Two internal genes - *GAPDH* (in case of RNA from tumor bulk) and *ACTB1* (RNA from the microdissected material) were used to normalize expression levels of the studied genes. The average C_t (cycle threshold) was estimated for both the gene of interest, *GAPDH*, and *ACTB1*. Relative expression was evaluated using the Pfaffl method⁴⁵, and the formula was used to determine the expression ratio between the sample and the calibrator¹⁵. The relative expression level was also normalized to a calibrator consisting of a pool of normal breast tissue specimens. For this purpose, specimens of adjacent normal breast tissue from 10 breast cancer patients (NAC-free) were used as a source of normal RNA. In case of the microdissected samples, we normalized the expression levels relative to normal breast tissue of the same patient. The results were presented as n-fold differences in MDR gene expression relative to *GAPDH/ACTB1* and normal breast tissue.

Statistics. Statistical analyses were performed using STATISTICA 8.0 software (StatSoft, Tulsa, OK, USA). The arithmetic mean value and standard error were calculated for each sample group. Logistic regression was applied to identify the link between pre-/post-NAC expression levels of MDR genes and the presence/absence of different types of morphological structures in breast tumors. Pearson's chi-square test was used to detect the association of NAC response and change (increase or decrease) in expression of MDR genes with the presence/absence of different types of morphological structures in breast tumors. The Bonferroni correction was applied to address the problem of multiple comparisons and was calculated as the each p value multiplied by the number of comparisons⁴⁶. The necessary to apply Bonferroni correction to the comparisons made was dictated by the confirmatory nature of this study with a clear prespecified key question consisting of several hypotheses analysed by multiple significance tests⁴⁷. P-values that were corrected to values more than 1 were truncated to 1. Differences were significant if the corrected p value was less than 0.05. All p values were two-sided.

1. Bertos, N. R. & Park, M. Breast cancer - one term, many entities? *J Clin Invest.* **121**, 3789–3796 (2011).
2. Ng, C. K., Pemberton, H. N. & Reis-Filho, J. S. Breast cancer intratumor genetic heterogeneity: causes and implications. *Expert Rev Anticancer Ther.* **12**, 1021–1032 (2012).
3. Lakhani, S. R., Ellis, I. O., Schnitt, S. J., Tan, P. H. & van de Vijver, M. J. *World Health Organization (WHO) classification of tumours of the breast, 4th ed* (IARC Press, Lyon, 2012).
4. Tavassoli, F. A. & Devile, P. *Pathology and Genetics of Tumours of the Breast and Female Genital Organs* (IARC Press, Lyon, 2003).
5. O'Malley, F. P., Pinder, S. E. & Mulligan, A. M. *Breast Pathology, 2nd ed.* (Elsevier, Philadelphia, 2011).
6. Goldschmidt, R. A. [Histopathology of malignant breast disease]. *Atlas of clinical oncology*. [Winchester, D. J. & Winchester, D. P. (eds.)]. [89–98] (B.C. Decker Inc., Hamilton, 2000).
7. Zavyalova, M. V. *et al.* The presence of alveolar structures in invasive ductal NOS breast carcinoma is associated with lymph node metastasis. *Diagn Cytopathol.* **41**, 279–282 (2013).
8. Perelmuter, V. M. *et al.* Genetic and clinical and pathological characteristics of breast cancer in premenopausal and postmenopausal women. *Adv Gerontol (Russian)*. **21**, 643–653 (2008).
9. Zavyalova, M. V. *et al.* Phenotypic drift as a cause for intratumoral morphological heterogeneity of invasive ductal breast carcinoma not otherwise specified. *BioResearch Open Access.* **2**, 148–154 (2013).

10. Bhatia, S., Frangioni, J. V., Hoffman, R. M., Iafrate, A. J. & Polyak, K. The challenges posed by cancer heterogeneity. *Nat Biotechnol.* **30**, 604–610 (2012).
11. Gerashchenko, T. S. *et al.* Intratumoral heterogeneity: nature and biological significance. *Biochemistry (Mosc)*. **78**, 1201–1215 (2013).
12. Zavyalova, M. V. *et al.* Relationship between tumor sensitivity to neoadjuvant chemotherapy and histologic pattern of primary tumor in unicentric infiltrating ductal breast carcinoma. *Siberian Journal of Oncology.* **6**, 30–34 (2008).
13. Stavrovskaya, A. A. & Stromskaya, T. P. Transport proteins of the ABC family and multidrug resistance of tumor cells. *Biochemistry (Moscow)*. **73**, 592–604 (2008).
14. Gottesman, M. M. Mechanisms of cancer drug resistance. *Annu Rev Med.* **53**, 615–627 (2002).
15. Litviakov, N. V. *et al.* Changing the expression vector of multidrug resistance genes is related to neoadjuvant chemotherapy response. *Cancer Chemother Pharmacol.* **71**, 153–163 (2013).
16. Litviakov, N. V. *et al.* Connection of metastasis-free survival in breast cancer patients and an expression vector of multidrug resistance genes in tumor during neoadjuvant chemotherapy. *Voprosy onkologii (Russ)*. **59**, 334–340 (2013).
17. Kim, B. *et al.* Neoadjuvant chemotherapy induces expression levels of breast cancer resistance protein that predict disease-free survival in breast cancer. *PLoS One.* **8**, e62766 (2013).
18. Denisov, E., Tsyganov, M., Tashireva, L., Zavyalova, M., Perelmuter, V. & Cherdynseva, N. Intratumoral heterogeneity in expression of chemotherapy response markers in invasive ductal breast carcinoma NOS. Paper presented at 4th WIN Symposium: Efficacy of biomarkers and personalized cancer therapeutics, Paris, France. *Ann Oncol.* **23**, v21–v22 (2012).
19. Rafii, A. *et al.* Stromal cells extracted from ovarian cancer express functional multi drugs resistance proteins: ATP binding cassette and Major vault protein. Paper presented at ASCO Annual Meeting, Atlanta, USA. *J Clin Oncol.* **24**, 2072 (2006).
20. Wishart, G. C. *et al.* P-glycoprotein expression in primary breast cancer detected by immunocytochemistry with two monoclonal antibodies. *Br J Cancer.* **62**, 758–761 (1990).
21. Linn, S. C. *et al.* Expression of drug resistance proteins in breast cancer, in relation to chemotherapy. *Int J Cancer.* **71**, 787–795 (1997).
22. Sutherland, R. M., Eddy, H. A., Bareham, B., Reich, K. & Vanantwerp, D. Resistance to adriamycin in multicellular spheroids. *Int J Radiat Oncol Biol Phys.* **5**, 1225–1230 (1979).
23. Durand, R. E. & Sutherland, R. M. Effects of intercellular contact on repair of radiation damage. *Exp Cell Res.* **71**, 75–80 (1972).
24. Durand, R. E. Adriamycin: a possible indirect radiosensitizer of hypoxic tumor cells. *Radiology.* **119**, 217–222 (1976).
25. Olive, P. L. & Durand, R. E. Drug and radiation resistance in spheroids: cell contact and kinetics. *Cancer Metastasis Rev.* **13**, 121–138 (1994).
26. Kobayashi, H., Man, S., Graham, C. H., Kapitain, S. J., Teicher, B. A. & Kerbel, R. S. Acquired multicellular-mediated resistance to alkylating agents in cancer. *Proc Natl Acad Sci U S A.* **90**, 3294–3298 (1993).
27. Desoize, B. & Jardillier, J. Multicellular resistance: a paradigm for clinical resistance? *Crit Rev Oncol Hematol.* **36**, 193–207 (2000).
28. Ivascu, A. & Kubbies, M. Diversity of cell-mediated adhesions in breast cancer spheroids. *Int J Oncol.* **31**, 1403–1413 (2007).
29. Moore, N. & Lyle, S. Quiescent, slow-cycling stem cell populations in cancer: a review of the evidence and discussion of significance. *J Oncol.* **2011**, (2011).
30. Mellor, H. R. & Callaghan, R. Accumulation and distribution of doxorubicin in tumour spheroids: the influence of acidity and expression of P-glycoprotein. *Cancer Chemother Pharmacol.* **68**, 1179–1190 (2011).
31. Doublier, S. *et al.* HIF-1 activation induces doxorubicin resistance in MCF7 3-D spheroids via P-glycoprotein expression: a potential model of the chemoresistance of invasive micropapillary carcinoma of the breast. *BMC Cancer.* **12**, 4 (2012).
32. Acs, G., Esposito, N. N., Rakosy, Z., Laronga, C. & Zhang, P. J. Invasive ductal carcinomas of the breast showing partial reversed cell polarity are associated with lymphatic tumor spread and may represent part of a spectrum of invasive micropapillary carcinoma. *Am J Surg Pathol.* **34**, 1637–1646 (2010).
33. Li, Y. S., Kaneko, M., Sakamoto, D. G., Takeshima, Y. & Inai, K. The reversed apical pattern of MUC1 expression is characteristics of invasive micropapillary carcinoma of the breast. *Breast Cancer.* **13**, 58–63 (2006).
34. Hou, J. M. *et al.* Circulating tumor cells as a window on metastasis biology in lung cancer. *Am J Pathol.* **178**, 989–996 (2011).
35. Yu, M., Stott, S., Toner, M., Maheswaran, S. & Haber, D. A. Circulating tumor cells: approaches to isolation and characterization. *J Cell Biol.* **192**, 373–382 (2011).
36. Stott, S. L. *et al.* Isolation of circulating tumor cells using a microvortex-generating herringbone-chip. *Proc Natl Acad Sci U S A.* **107**, 18392–18397 (2010).
37. Brandt, B. *et al.* Isolation of prostate-derived single cells and cell clusters from human peripheral blood. *Cancer Res.* **56**, 4556–4561 (1996).
38. Kats-Ugurlu, G. *et al.* Circulating tumour tissue fragments in patients with pulmonary metastasis of clear cell renal cell carcinoma. *J Pathol.* **219**, 287–293 (2009).
39. Murray, N. P., Vidal Albarran, R.-C., Pérez O, G., Ruiz M, A., Porcell E, J. & Castillo A, A. M. Cytomorphology of circulating tumor cells and cell clusters in Chilean patients with colo-rectal cancer. *Int J Morphol.* **30**, 834–839 (2012).



40. Molnar, B., Ladanyi, A., Tanko, L., Sreter, L. & Tulassay, Z. Circulating tumor cell clusters in the peripheral blood of colorectal cancer patients. *Clin Cancer Res.* **7**, 4080–4085 (2001).
41. Greene, B. T., Hughes, A. D. & King, M. R. Circulating tumor cells: the substrate of personalized medicine? *Front Oncol.* **2**, 69 (2012).
42. Hou, J. M. *et al.* Clinical significance and molecular characteristics of circulating tumor cells and circulating tumor microemboli in patients with small-cell lung cancer. *J Clin Oncol.* **30**, 525–532 (2012).
43. Hayward, J. L., Carbone, P. P., Heuson, J. C., Kumaoka, S., Segaloff, A. & Rubens, R. D. Assessment of response to therapy in advanced breast cancer: a project of the Programme on Clinical Oncology of the International Union Against Cancer, Geneva, Switzerland. *Cancer.* **39**, 1289–1294 (1977).
44. Nishimura, M., Yoshitsugu, H., Naito, S. & Hiraoka, I. Evaluation of gene induction of drug-metabolizing enzymes and transporters in primary culture of human hepatocytes using high-sensitivity real-time reverse transcription PCR. *Yakugaku Zasshi.* **122**, 339–361 (2002).
45. Pfaffl, M. W. A new mathematical model for relative quantification in real-time RT-PCR. *Nucleic Acids Res.* **29**, e45 (2001).
46. Rice, W. R. Analyzing tables of statistical tests. *Evolution.* **43**, 223–225 (1989).
47. Bender, R. & Lange, S. Adjusting for multiple testing--when and how? *J Clin Epidemiol.* **54**, 343–349 (2001).
48. Wolff, A. C. *et al.* American Society of Clinical Oncology/College of American Pathologists guideline recommendations for human epidermal growth factor receptor 2 testing in breast cancer. *Arch Pathol Lab Med.* **131**, 18–43 (2007).

Acknowledgments

The study was supported by The Ministry of education and science of Russian Federation (projects 8291 and 8595), the Russian Federation President Grants (projects 16.120.11.1259-MK and 14.122.13.491-MD), and a grant from the OPTEK company (project 1/11KTS).

Author contributions

N.V.L., E.V.D., V.M.P. and N.V.C. designed the study. M.V.Z., S.V.V., E.Yu.G. and E.M.S. collected the tumor samples and the patient records. N.V.L., E.V.D., M.V.Z., S.V.V., M.M.T. and T.S.G. performed the experiments. N.V.L., E.V.D., M.V.Z. and T.S.G. analysed and statistically processed the data. N.V.L. and E.V.D. wrote the paper. E.M.S., V.M.P. and N.V.C. assisted in critiquing, editing, and refining the paper. All authors reviewed the manuscript.

Additional information

Competing financial interests: The authors declare no competing financial interests.

How to cite this article: Denisov, E.V. *et al.* Intratumoral morphological heterogeneity of breast cancer: neoadjuvant chemotherapy efficiency and multidrug resistance gene expression. *Sci. Rep.* **4**, 4709; DOI:10.1038/srep04709 (2014).



This work is licensed under a Creative Commons Attribution-NonCommercial-NoDerivs 3.0 Unported License. The images in this article are included in the article's Creative Commons license, unless indicated otherwise in the image credit; if the image is not included under the Creative Commons license, users will need to obtain permission from the license holder in order to reproduce the image. To view a copy of this license, visit <http://creativecommons.org/licenses/by-nc-nd/3.0/>